Electrophysical Modelling and Analysis of Activity in Neurons

Atsushi Fukasawa
Former Professor, Chiba University, JAPAN
fukasawafuji@yahoo.co.jp

Yumi Takizawa
Institute of Statistical Mathematics, JAPAN
takizawa@ism.ac.jp

Abstract: - This paper presents electrophysical activity in neurons. Electrophysical activity is analysed by motion of charges (ions) in time and space (zones). Dynamic modelling is composed of three electrical zones and two depletion layers (liquid junctions) induced in cytoplasm. This paper then presents that positive pulse is realized by this model as the typical output, and that negative pulse, positive and negative plateaus are realized as the variations depending on ion channels in receptors driven by the first and the second messengers. It is concluded that commonality in scheme and variation in output potentials exist in neurons.

Key-Words: - Electrophysical activity, liquid junction, zone and depletion layer, positive pulse as typical output, negative pulse/positive - negative plateaus as variation, the first and the second messengers.

1 Introduction

It has been thought that neurons generate positive pulses for input stimulations. Fundamental scheme is asked of activity in neurons by the authors [1-10]. It is hard to observe isolated operation of a single neuron in neural networks.

Unicellular organisms are taken into the study to find essential scheme of excitation. It is noted that bipolar (positive and negative) potentials in *noctiluca* are used (a) for motion control of tentacle, and (b) with Na^+ and Cl^- channels [11]. It was shown that bipolar potentials are used (c) for motion control of cilia, but (d) with Ca^{2+} and K^+ channels [5,7].

It was also reported that bipolar potential outputs were observed in neuron of *aplysia* by R. MacCaman, 1982[12], and M. Shouzushima, 1984[13]. Biochemical process of G-protein for the secondary messengers were studied by K. Sasaki, et al, 1987[14] with positive and negative post synaptic potentials.

This paper presents a unified modelling of activity in neurons. This model is composed of electrical three zones and two depletion layers induced in cytoplasm.

This paper then presents that typical output of this model is positive pulse. And the variations are negative pulse, positive and negative plateaus depending on ion channels in receptors driven by the first and the second messengers.

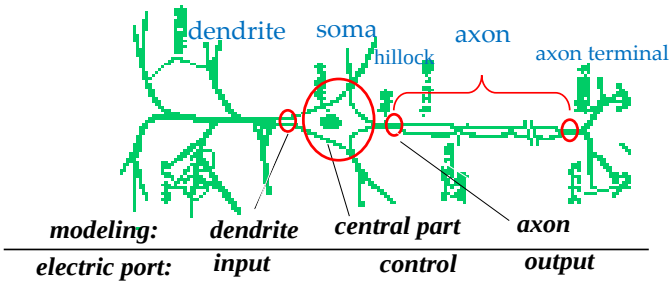

Fig. 1 Schematic diagram of a neuron.

2 Electro-physical Modelling for Positive Potential Generation

2.1 Schematic diagram and electrophysical configuration

Schematic diagram of a neuron is shown in Fig.1. Dendrites, soma, and axon are actual components of a living neuron. Dendrite, central part, and axon are newly defined for analysis, and they correspond to input, control, and output of response of an active neuron.

Electrophysical model of an active neuron is shown in Fig. 2. Zones and boundaries are formulated in cytoplasm corresponding to each component.

In Fig. 2, receptor is composed of a set of three components (regulatory and catalytic subunits, and G-protein) and Na^+ channels. When neurotransmitter is received by the former, it produces the second messenger (c-AMP, c-DMP, etc.) and drives to open Na^+ channels indirectly.

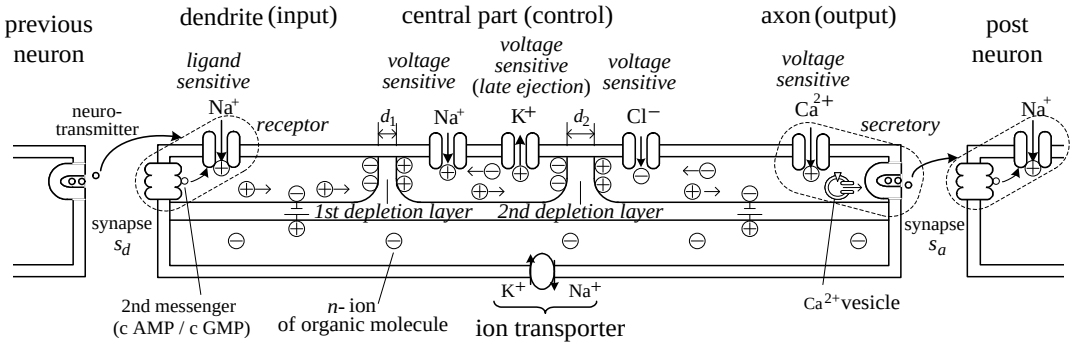

Fig. 2 Electro-physical modelling for positive potential generation.
Na^+ channels at the dendrite are ligand-dependent. Na^+ channels at the central part are voltage dependent. Ejection of K^+ at the central part reduces pulse-width by rapid return to resting potential. Injection of Cl^- at the axon and its current flow to the left contribute to current multiplication. Na^+ - K^+ transporter works as a battery.

When neurotransmitter is received by the latter, the Na^+ channel are opened directly by the neurotransmitter.

Na^+ ions distribute in thin layer under the membrane, because the quantity of total ions are very poor to fulfil whole cross section of cytoplasm. Cl^- channels must be distributed at axon to increase total amount of current to meet condition of oscillation.

Secretory emits neurotransmitter to post neuron by exocytosis with Ca^{2+} ions.

2.2 Energy diagram of charges (ions)

Corresponding to Fig.2, energy vs position in *z* axis (energy diagram) is shown in Fig. 3.

The Fermi level is shown by a solid line for mean energy of positive (*p*-) and negative (*n*-) ions. Energy difference of *p*- and *n*-ions is estimated to be small in electrolyte.

The energy at the dendrite becomes high by injection of Na^+ ions (signal *p*-ions). By injection of *p*-ions at the central part, the energy becomes low corresponding to wall potential reduction. Early potential return to resting state by late ejection of K^+ at the central part yield a narrow pulse. This process is exhibited equivalently by the forward diode.

Carrier *p*-ions drift in the central part with flat potential. At the second boundary, potential wall is higher at the second depletion layer. A little charges pass over the potential wall with energy enhancing by thermal motion.

The current multiplication is realized by additive negative current by Cl^- ions.

Pulse oscillation is made by a single neuron.

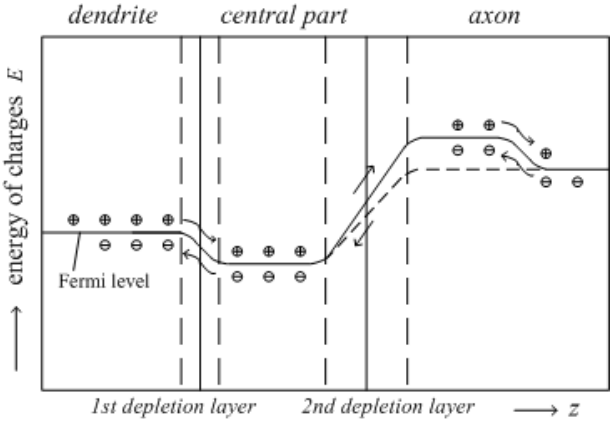

Fig. 3 Energy diagram of positive and negative ions. Cl^- channels at the axon works as a current multiplier. If Cl^- channels are deleted from the axon, energy *E* is reduced as shown by dotted line.

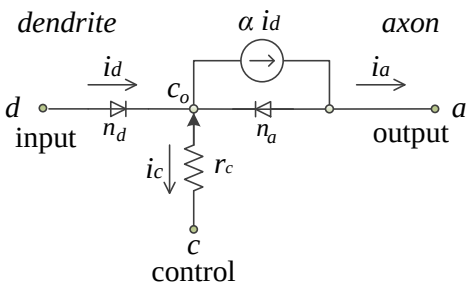

Fig. 4 Electrical modelling of activity of a neuron for positive potential generation.

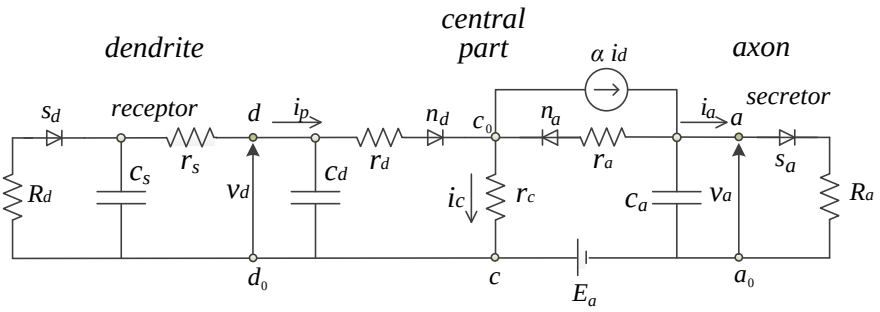

Fig.5 Equivalent circuit of a neuron for positive potential generation.
Receptor is expressed by charge-discharge c_s - r_s circuit.

2.3 Equivalent circuit of activity

Corresponding to the energy diagram in Fig. 3, an equivalent circuit of activity is shown in Fig. 4 for positive potential generation.

Forward and reverse diodes n_d and n_a denote positive charge dynamics at the first and the second depletion layers respectively.

Points *d*, *c*, and *a* denote input (dendrite), control, and output (axon) ports. c_0 is a virtual point corresponding to average potential in the central part.

$\alpha \cdot i_d$ is the equivalent current source to drive the output load. α is current multiplication factor for i_d.

r_C is diffusion resistance at the central part.

Most of input current i_d reaches *a*. Current i_c is defined by components of input i_d and feedback of output current i_a.

3 Electrical Characteristics

3.1 Equivalent circuit of total neuron

The total equivalent circuit of a neuron is shown in Fig.5 for positive potential generation. Activity is given by a section between *d* - d_0 and *a* - a_0.

The capacities c_d and c_a are fundamentally defined by induced capacities at the first and the second depletion layers. Practically membrane capacity is added to them, but it is ignored in the analysis.

The equivalent circuit of input synapse and chemical process of receptor are shown by a voltage source and a charge-discharge c_s - r_s circuit. This circuit defines the effects of the first-messenger-driven ion channels and the second-messenger (cAMP, cGMP, etc.)-driven ion channels.

The equivalent circuit of chemical process of secretory and output synapse are shown by the road resistance.

Impedances r_d and r_a of forward and reverse diodes n_d and n_a are low and high resistances respectively. Impedance ratio r_a / r_d is kept large enough to limit coupling of output to input circuits.

Input and output synapses s_d and s_a.are shown as forward diodes for excitatory synapses (*p*-ions). Potential E_a is derived with an ion transporter (ion pump) in Fig. 2.

3.2 Characteristics as an amplifier

When reverse diode resistance $r_a \approx \infty$ approximately, closed loop gain G_v, open loop gain *K*, and feedback ratio β are given as follows.

$$G_v = \frac{v_a}{v_d} = \frac{\dfrac{\alpha R_a}{r_d + r_c}}{1 - \dfrac{\alpha R_a}{r_d + r_c} \cdot \dfrac{r_c}{R_a}} = \frac{K}{1 - K\beta} \qquad (1)$$

$$K = \alpha \frac{R_a}{r_d + r_C} \qquad (2)$$

$$\beta = \frac{r_C}{R_a} \qquad (3)$$

where, v_d and v_a are input and output voltages of a neuron, G_v, *K*, β are closed loop gain, open loop gain, and inner feedback ratio of a neuron respectively. Oscillation condition is given by $K\beta \geq 1$. (ref. Appendix A-3)

In case that the axon has few Cl channels, $\alpha < 1$, $K\beta << 1$. Therefore a neuron operates as an amplifier with threshold for input signal with positive inner feedback.

Negative current flows to the left by injection of Cl^- charges.

The energy (power) gain G_E is given by;

$$G_E = G_v G_c \quad (4)$$

Where, *Gc* is current gain by sum of positive and negative currents flowing to the right.

Even if input stimulation could not exceed the threshold, a certain information is transmitted to the axon terminal and to the posit neurons. It is found in this paper that this effect is explained by amplification by a neuron.

3.3 Operational Characteristics as an oscillator

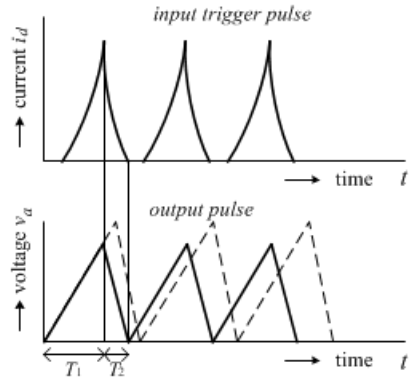

Fig.6 Output voltage waveform for positive potential generation. The dotted line is an original waveform. The solid line is synchronized waveform to the input trigger pulse.

(1) Pulse oscillator

The neuron operates as a pulse oscillator to generate the output of potential waveforms when the product of open loop gain *K* and feedback ratio β exceeds 1.

This oscillator is composed of self-injection with inner feedback signal without external trigger.

$$T_1 = c_d \frac{r_c R_a}{r_c + R_a} \quad (5)$$

$$T_2 = c_a R_a \quad (6),$$

where, $R_d + r_d >> r_c$, $r_a = \infty$ are assumed for simplified analysis.

The period of oscillation *T* is given as the total time length as following;

$$T = T_1 + T_2 = C_d \frac{r_c R_a}{r_c + R_a} + C_a R_a \quad (7).$$

The mode of oscillation is astable. The stable point is only at the bottom.

The neuron operates as an astable mode tuned to external injection. Whenever, the phase and the period of original free running oscillator is fluctuating, the oscillator becomes stable by locking to the external signal as shown in Fig. 6.

Synchronization is established in a system with a group of neurons, and a stable timing clock is realized by total coupling among neurons.

(2) Plateau oscillator

When the ion channel in the receptor is composed of a secondary messenger, the input signal is featured by a long holding time defined by discharge effects.

$$T_3 \approx c_s (r_s + r_c) + c_d \frac{r_c R_a}{r_c + R_a} \quad (8),$$

$$T_4 = c_a R_a \quad (9).$$

where, $r_d << r_c$, $c_d << c_s$

The period of oscillation *T* with pulse and plateau is given as the total time length as following (Fig. 7).

$$T = T_1 + T_2 + T_3 + T_4 \quad (10)$$

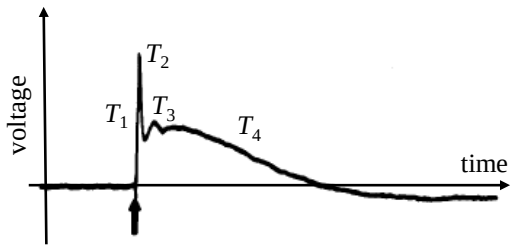

Fig. 7 Typical output voltage with positive pulse and plateau.

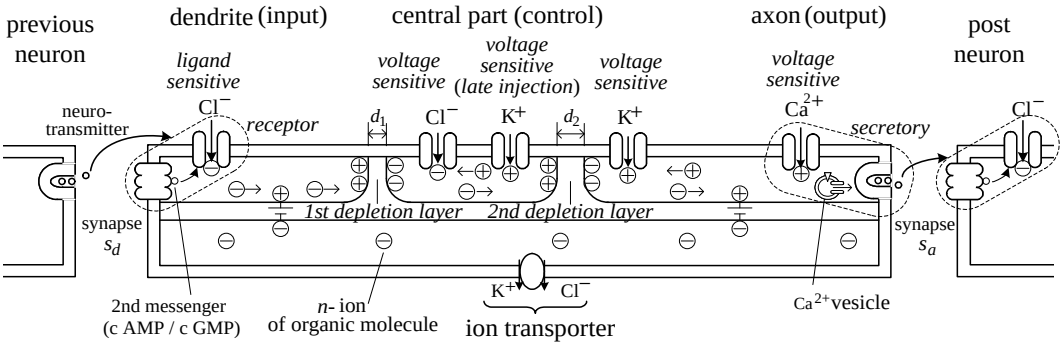

Fig. 8 Electro-physical modelling of an active neuron for negative potential generation. Cl^- channels at the dendrite is ligand-dependent. Cl^- channels at the central part are voltage dependent. K^+ channels at the central part and at the axon contribute to reduction of pulse width and current multiplication respectively.

4 Characteristic of an Active Neuron for Negative Potential Generation

4.1 Equivalent circuit of total neuron

Electro-physical modelling of a neuron for negative potential generation is given in Fig. 8.

Formation of zones and depletion layers in Fig. 8 is same to Fig. 2 except the kinds of ion channels. Ion channels for reception of signals from previous neurons are ligand-dependent Cl^- channels

Ion channels for reception of signals from previous neurons are ligand dependent Cl^- channels. Cl^- and K^+ channels at the central part and at the axon are voltage dependent. Ca^{2+} channels are provided for secretion of neurotransmitters.

K^+ and Cl^- transmitters operate to provide resting potential which works as a battery for neural circuit [17].

4.2 Electrical Characteristics

Electrical modelling of the activity for negative potential generation is shown in Fig. 9. Input and output diodes n_d, n_a correspond to the first and the second depletion layers, which are shown as reverse and forward diodes respectively.

Equivalent circuit of an active neuron is shown in Fig. 10 for negative potential generation.

For negative potential generation, the waveform is just inverse of the waveform shown in Fig. 6 and 7.

It is summarized that modelling and analysis of electrical characteristics are common to neurons with positive and negative potential outputs except the direction of diodes and current flows in the equivalent circuit.

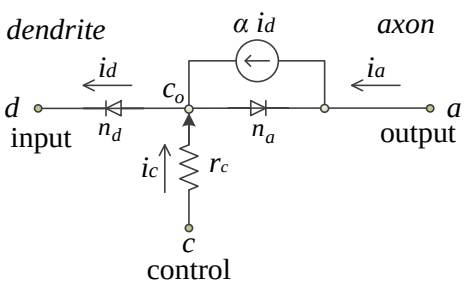

Fig. 9 Electrical modelling of activity of a neuron for negative potential generation.

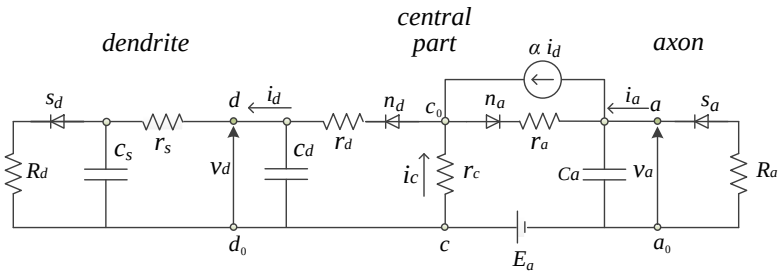

Fig. 10 Electrical modelling of an active neuron for negative potential generation.

5 Conclusion

Unified modelling of activity in neurons was given in this paper. By this modelling, typical potential output is positive pulse. And the variations in output potentials are negative pulse, positive and negative plateaus depending on ion channels in the receptor driven by the first and the second messengers. These output potentials depend on conditions of marine, limnetic, and physiological solutions in nature.

References:

[1] Fukasawa A., Takizawa Y., Activity of a Neuron and Formulation of a Neural Group for Synchronization and Signal Processing, *Proc. of the Int. Conf. on Neurology*, pp.242-247, Kos, Greece, July 2012, *"The Best Paper Prize of NEUROLOGY'12" awarded by WSEAS/NAUN*.

[2] Fukasawa A. Takizawa Y., Activity of a Neuron and Formulation of a Neural Group for Synchronized Systems, *International Journal of Biology and Biomedical Engineering*, Issue 2, vol. 6, pp. 149-156, 2012.

[3] Fukasawa A., Takizawa Y., Activity of a Neuron and Formulation of a Synchronous Neural System, *Proc. on International Conference on Mathematical Methods, Computational Techniques and Intelligent Systems (MAMECTIS'13)*, pp. 66-73, 2013.

[4] Fukasawa A., Takizawa Y., Activity of a Neuron and Formulation of a Neural Group based on Mutual Injection in keeping with system synchronization, *Proc. of International conference on Circuit, Systems, Control, Signals (CSCS'12)*, pp. 53-58, Barcelona, Spain, Oct. 17, 2012.

[5] Takizawa Y., Fukasawa A., Takeuchi H-. A., Positive and Negative Action Potentials in Paramecium Relating to Neurons, *Proc. of International Conference on Health Science and Biomedical Systems (HSBS'15)*, pp.54-60, Aug., 2015.

[6] Fukasawa A., Takizawa Y., Activity of a Neuron for Generation of Pulse and Plateau with Positive and Negative Potentials, *Proc. of International Conference on Health Science and Biomedical Systems (HSBS'15)*, pp.65-71, Aug., 2015.

[7] Takizawa Y., Fukasawa A., Takeuchi H-.A., Excitation of Paramecium with Membrane Potential Generation for Swimming Direction by Cilia, WSEAS Transactions on Biology and Biomedicine, vol.12, pp.62-68, 2015.

[8] Takizawa Y., Fukasawa A., Natori K., Excitation of a Neuron for Characteristic Potential Generation, WSEAS Transactions on Biology and Biomedicine, vol.12, pp.62-68, 2015. vol.12, pp.69-78, 2015.

[9] Fukasawa A., Takizawa Y., Modelling of a Neuron and Point Contact Transistor, *International Journal of Biology and Biomedical Engineering*, vol.9, pp.14-21, 2015.

[10] Fukasawa A., The latest Studies of Activities in Neuron and Unicellular Organism, Plenary Lecture, *Proc. of International Conference on HSBS'16*, Ischia, Italy, June 17-19, 2016.

[11] Oami K., Sibaoka T. and Naitoh Y., Tentacle regulating potentials in Noctiluca miliaris: their generation sites and ionic mechanisms, *J. Comp. Physiol.* A 162, pp. 179-185, 1988.

[12] MacCaman R. E., Weinreich D., On the nature of histamine mediated slow hyperpolarizing synaptic potentials in identified molluscan neurons, *Journal of Physiol.*, 328, pp. 485-506, 1982.

[13] Shozushima M, Blocking Effect of Serotonin on Inhibitory Dopamine Receptor Activity of *Aplysia* Ganglion Cells, *Japanese Journal of Physiology*, 34, pp. 225-243, 1984.

[14] Sasaki K., et al, A single GTP-binding protein regulates K^+-channels couples with dopamine, histamine and acetylcholine receptors, *Nature*, Fig. 1, 325, 259, 1987.

[15] Takizawa Y., Fukasawa A., Electrophysical Modelling and Analysis of Axon in Neurons, *Proc. of International Conference on HSBS '16*, June 17-19, 2016.

[16] Shockley W., *Electrons and holes in semiconductors*, Fig. 4-13, pp. 112-113, D. Van, Nostrand, New York, 1950.

[17] Okada Y., Ion channels and Transporters Involved in Cell Volume Regulation and Sensor mechanisms, *Cell Biochemistry and Biophysics*, vol.41, pp.233-257, 2004.

[18] Takizawa Y., Fukasawa A., Formulation of Topographical Mapping in Brain with a Synchronous Neural System, *Proceedings of the 15th International Conference on Mathematical Methods, Computational Techniques and Intelligent Systems (MAMECTIS'13)*, pp. 60–65, Lemesos, Cyprus, Mar. 21-23, 2013.

[19] Takizawa Y., Fukasawa A., Formulation of a Neural System and Analysis of Topographical

Mapping in Brain, *International Journal of Biology and Biomedical Engineering*, Issue 2, vol. 6, pp. 157-164, 2012.
[20] Takizawa Y., Fukasawa A., Electrical Measurement Scheme of Liquid Boundaries in Active Neuron, *Proc. of Int. Conf. on Health Science and Biomedical Systems (HSBS'14)*, pp. , Nov. 22, 2014.
[21] Catsigeras E., Self-synchronization of networks with a strong kernel of integrate and fire excitatory neurons, *WSEAS Transactions on Mathematics*, Issue 7, Vol. 12, Section 5, p. 794, July 2013.
[22] Takizawa Y., Rose G., Kawasaki M., Resolving Competing Theories for Control of the Jamming Avoidance Response: The Role of Amplitude Modulations in Electric Organ Discharge Decelerations, *Journal of Exp. Biol.* 202, pp. 1377-1386, 1999.

Appendix

A1. Formation of depletion layer (liquid junction)

It is considered that positive (*p*–) ions are injected into uniform electrolyte filled with negative (*n* –) ions. *p* - ions diffuse to *n* - side by the gradient of density. *n* – ions diffuse to *p* – side simultaneously. Coulomb's force appears between diffused *p*- and *n*-charges. When diffusion and Coulomb's forces are balanced, diffusion stops as shown in Fig. A-1(a).

Depending on the difference of potentials in *p*- and *n*-zones, a potential wall appears with space charges distributed at each side of space as shown in Fig. A-1(b). If any charges are in the space, they are driven out of the space. This is denoted a depletion layer.

The equational analysis is written in [3].

A glass electrode is inserted into the cytoplasm of a test cell. When the cytoplasm and solutions in the electrode are different, the potential difference appears between true and experimental observations. This effect is well known in solid (semiconductor) and liquid sciences.

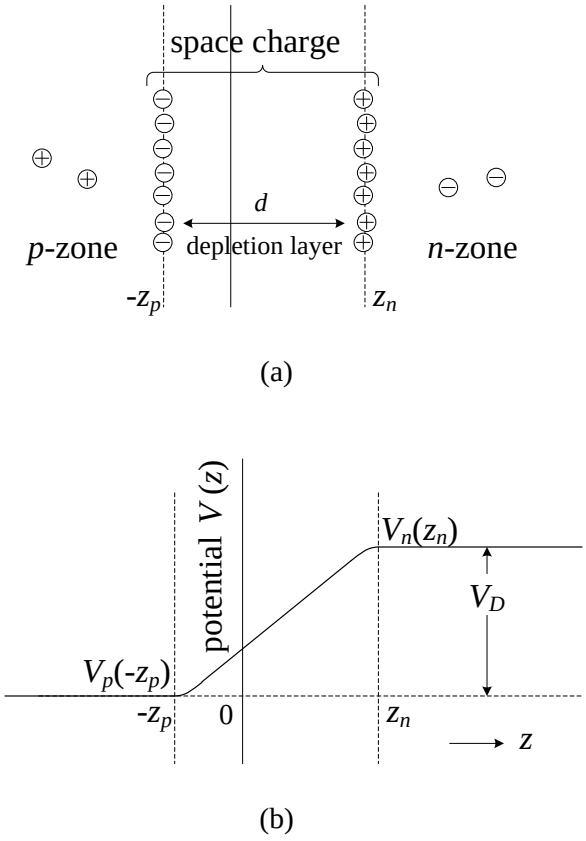

Fig. A-1 Depletion layer (liquid junction) composed of space charge and potential difference at a *p* – *n* boundary.
(a) Space charge distribution
(b) Potential difference